This article was downloaded by:
On: *26 January 2011*
Access details: *Access Details: Free Access*
Publisher *Taylor & Francis*
Informa Ltd Registered in England and Wales Registered Number: 1072954 Registered office: Mortimer House, 37-41 Mortimer Street, London W1T 3JH, UK

Liquid Crystals
Publication details, including instructions for authors and subscription information:
http://www.informaworld.com/smpp/title~content=t713926090

Influence of boundary conditions on electrooptical and magnetooptical effects in nematics

U. D. Kini[a]
[a] Raman Research Institute, Bangalore, India

To cite this Article Kini, U. D.(1993) 'Influence of boundary conditions on electrooptical and magnetooptical effects in nematics', Liquid Crystals, 13: 6, 735 — 755
To link to this Article: DOI: 10.1080/02678299308027290
URL: http://dx.doi.org/10.1080/02678299308027290

PLEASE SCROLL DOWN FOR ARTICLE

Full terms and conditions of use: http://www.informaworld.com/terms-and-conditions-of-access.pdf

This article may be used for research, teaching and private study purposes. Any substantial or systematic reproduction, re-distribution, re-selling, loan or sub-licensing, systematic supply or distribution in any form to anyone is expressly forbidden.

The publisher does not give any warranty express or implied or make any representation that the contents will be complete or accurate or up to date. The accuracy of any instructions, formulae and drug doses should be independently verified with primary sources. The publisher shall not be liable for any loss, actions, claims, proceedings, demand or costs or damages whatsoever or howsoever caused arising directly or indirectly in connection with or arising out of the use of this material.

LIQUID CRYSTALS, 1993, VOL. 13, NO. 6, 735–755

Influence of boundary conditions on electrooptical and magnetooptical effects in nematics

by U. D. KINI
Raman Research Institute, Bangalore, 560 080, India

(*Received 28 August 1992; accepted 27 January 1993*)

The continuum theory is used to study a polar electrooptic effect in a nematic insulator which is caused by applying an electric field normal to the sample planes having different director anchoring strengths. In the low field limit the magnitude of the linear electrooptical effect is studied as a function of anchoring strengths, director tilt at the boundaries, magnitude of flexoelectric constants and an applied magnetic field. The effect becomes stronger with increasing flexoelectricity or a stabilizing magnetic field and becomes weaker with a destabilizing magnetic field, pretilt of the initial director away from the homogeneous orientation or increase in sample thickness. As in the case of the Fréedericksz threshold, the magnitude of the applied voltage at which the director field orients along the sample normal is found to depend on the sign of the voltage as a consequence of unequal anchoring strengths and flexoelectricity. Under the rigid anchoring hypothesis the mathematical model is extended to study magnetic field induced bistability. It is found that the bistability width as well as the associated optical properties of the nematic sample can be profoundly influenced by the application of an electric field.

Downloaded At: 11:44 26 January 2011

1. Introduction

The success of the continuum theory [1–7] lies mainly in its ability to account for a number of fascinating and useful phenomena which occur under the action of external electric and magnetic fields on nematics. Due to the anisotropy of susceptibilities of these materials, external fields can influence the preferred direction of orientation represented by the unit, non-polar director field, **n**. The magnetic and electric Fréedericksz transitions are useful for estimating the curvature elastic constants of nematics. The field effects are comparatively straightforward to interpret in the case of an imposed magnetic field as the field inside the sample is not appreciably distorted by the director gradients owing to the rather small magnitude of the diamagnetic susceptibility anisotropy (χ_A). As the diamagnetic free energy density depends on the square of the field strength and also because of the non-polar nature of the director field the sign of the magnetic field does not need to be considered explicitly.

On the other hand, electric field effects are more complex and interesting. As the dielectric susceptibilities of a nematic are high it is necessary to take account of the distortion of the electric field inside the sample caused by director gradients [7]. The effects of flexoelectricity [8] can become prominent especially when the director anchoring strengths at the sample planes are not high [9, 10]. As the flexoelectric polarization couples linearly with the electric field the manifestation of flexoelectric influence generally occurs via a polar or linear electrooptical effect in those cases where optical observations are made. Such effects [11] formed the basis of some of the earliest

0267-8292/93 $10·00 © 1993 Taylor & Francis Ltd.

estimates of the flexoelectric constants and were subsequently refined by other investigators in later experiments [12].

One of the interesting polar electric effects was discovered by Derzhanski *et al.* [13] who showed that as a consequence of flexoelectricity the Fréedericksz threshold, V_S, in the splay geometry (electric field applied normal to the plates with initial director orientation parallel to the plates) can have different magnitudes when the sign of the applied voltage is reversed provided that the director anchoring strengths at the sample boundaries are different; these authors extended their study to various other cases.

One of the consequences of this polar electric effect is that sufficiently above the Fréedericksz threshold, a reversal in the sign of voltage should lead to a change in the average deformation and hence, also, a change in other average properties such as optical birefringence, intensity of light transmitted by the sample kept between crossed polarizers, etc. This follows directly from the fact that the splay Fréedericksz transition is one of second order and that the value of the average deformation at a voltage V essentially measures how much removed V is from V_S; naturally, under a reversal of sign of V, the difference $|V|-|V_S|$ will be different.

A facet of this electrooptic effect was recently demonstrated by Lee and Patel [14]. By making optical observations on a sample in the splay geometry with different anchoring strengths at the two substrates they showed that when the voltage is sufficiently high the change in optical path difference under reversal of sign of voltage is proportional to the difference in the anchoring strengths. They also obtained theoretical results in good agreement with experimental observations by employing a simple mathematical model.

It should be interesting to study how the magnitude of this linear electrooptical effect varies in the voltage region close to the splay threshold and what sort of dependence it has on the anchoring strengths and also other parameters such as director tilts at the boundaries and a magnetic field.

In addition to continuous orientational changes such as those considered above, discontinuous transitions between different deformation states have also been studied. For instance, the occurrence of a first order Fréedericksz transition has been reported [15] and possible effects of sample geometry, boundary conditions and an applied magnetic field have been theoretically studied [15, 16]. Bistability associated with a change of magnetic tilt has also been the subject of some past [17] as well as recent work [18, 19]. While the magnetic field strength is an important factor in determining the existence of bistability [17, 18], it has also been shown [19] that the bistability width (the range of magnetic tilt over which there exist two different deformation states with different free energy) can depend strongly on director anchoring strengths, director pretilts at the substrates, tilt of the magnetic plane, electric field applied along the sample planes, etc. In these works the average optical properties of the sample have not been studied in detail.

It seems instructive to find out how the optical properties of a nematic cell (for instance, intensity of light transmitted between crossed polarizers) change when the magnetic tilt is varied in small steps in a fixed plane and how an electric field applied normal to the sample planes can influence the occurrence of bistability.

With the above motivation, the governing equations and relevant boundary conditions are presented in § 2. § 3 contains results on the polar electric effect caused by asymmetric anchoring at the sample boundaries. In § 4 the rigid anchoring hypothesis is employed to study magnetic field induced bistability and the influence of an electric field applied normal to the plates. § 5 concludes the discussion.

Downloaded At: 11:44 26 January 2011

2. The mathematical model, governing equations and boundary conditions

The method suggested in [7, 10] is followed including the effect of an external magnetic field. Consider a nematic confined between sample planes $z = \pm h$ such that the easy axes at the plates are given by $d_\pm = (\cos\theta_\pm, 0, \sin\theta_\pm)$, respectively. The inside surfaces of the sample planes are assumed to have a (transparent) conducting coating to facilitate application of a potential difference. A magnetic field $\mathbf{H} = (H\cos\alpha, 0, H\sin\alpha)$ is impressed in the xy plane. If we concentrate on a region of the sample far away from the lateral edges it is reasonable to expect that under the joint actions of $\mathbf{H}$ and the electric field $\mathbf{E}$ the director field will be homogeneously deformed in the xz plane such that

$$\mathbf{n} = (C_\theta,\ 0,\ S_\theta);\quad C_\theta = \cos\theta(z);\quad S_\theta = \sin\theta(z). \tag{1}$$

Let $B_{\theta\pm}$ be the splay anchoring strengths at $z = \pm h$. Then the surface free energy density is [9].

$$\left.\begin{aligned} &W_S = \tfrac{1}{2}B_{\theta+}\sin^2(\theta_2 - \theta_+) + \tfrac{1}{2}B_{\theta-}\sin^2(\theta_1 - \theta_-);\\ &\theta_2 = \theta(z = +h);\quad \theta_1 = \theta(z = -h) \end{aligned}\right\} \tag{2}$$

As the anchoring energy at the sample boundaries is finite the orientation of $\mathbf{n}$ at a given plate will not coincide with that of the easy direction.

In general the electric field inside the sample can be written as

$$\mathbf{E} = [E_x(z),\ E_y(z), E_z(z)].$$

With the nematic assumed to be a perfect insulator, $\mathbf{E}$ is derivable from a potential so that Maxwell's curl equations [20] reduce to curl $\mathbf{E} = 0$, implying that E_x, E_y are constants. As per the boundary conditions which have to be satisfied at the interface between a dielectric and a conductor [20] the tangential components of $\mathbf{E}$ have to vanish at $z = \pm h$, so that $E_x = 0$, $E_y = 0$ in the sample and $\mathbf{E} = [0, 0, E_z(z)]$. In the absence of free charges the divergence equation of Maxwell (div $\mathbf{D} = 0$; $\mathbf{D}$ is the electric displacement) reduces to

$$D_z = \epsilon_0(\epsilon_\parallel S_\theta^2 + \epsilon_\perp C_\theta^2)E_z + (e_1 + e_3)S_\theta C_\theta \theta_{,z} = D_0, \tag{3}$$

where D_0 is a constant; ϵ_0 is the permittivity of free space; $\epsilon_{\parallel,\perp}$ are the dielectric constants of the nematic parallel to and normal to the director, respectively; $e_{1,3}$ are flexoelectric coefficients and a subscripted comma denotes differentiation with respect to z. With the definition $E_z = -\phi_{,z}$ where ϕ is the electric potential

$$V = \phi(+h) - \phi(-h) = -\int_{-h}^{h} E_z\, dz. \tag{4}$$

It will be seen that the sign of V, the potential difference, is important. Using equations (3) and (4) we can write

$$\left.\begin{aligned} &V = \psi - (D_0/\epsilon_0)\Gamma;\quad \psi = [(e_1 + e_3)/2\epsilon_0\epsilon_A]\ln[\epsilon_{zz}(\theta_2)/\epsilon_{zz}(\theta_1)];\\ &\epsilon_{zz}(\theta) = \epsilon_\parallel S_\theta^2 + \epsilon_\perp C_\theta^2;\quad \Gamma = \int_{-h}^{h} dz \Big/ \epsilon_{zz}(\theta), \end{aligned}\right\} \tag{5}$$

where $\epsilon_A = \epsilon_\parallel - \epsilon_\perp$ is the dielectric anisotropy. If V is held constant then the total thermodynamic potential density can be written as

$$\left.\begin{aligned} &W = \tfrac{1}{2}[K(\theta)\theta^2{}_{,z} - g(\theta) - D_0^2/\epsilon_0\epsilon_{zz}(\theta)];\quad g(\theta) = \mu_0\chi_A H^2\cos^2(\alpha - \theta);\\ &K(\theta) = K_1 C_\theta^2 + K_3 S_\theta^2 + (e_1 + e_3)^2 S_\theta^2 C_\theta^2/\epsilon_0\epsilon_{zz}(\theta); \end{aligned}\right\} \tag{6}$$

Downloaded At: 11:44 26 January 2011

χ_A is the diamagnetic susceptibility anisotropy and μ_0 the permeability of free space. If each sample plate has area A, the total thermodynamic potential per unit area

$$F'' = \int_{-h}^{h} W dz + W_S \tag{7}$$

is minimized with respect to variations of θ keeping V constant. Then the following governing equations and boundary conditions result:

$$\left.\begin{aligned} K(\theta)\theta_{,zz} + \tfrac{1}{2}(dK/d\theta)\theta_{,z}^2 + \tfrac{1}{2}(dg/d\theta) + D_0^2\epsilon_A S_\theta C_\theta/\epsilon_0\epsilon_{zz}^2(\theta) = 0; \\ K(\theta_2)(d\theta/dz)_{z=h} + \tfrac{1}{2}[B_{\theta+}\{\sin(2\theta_2 - 2\theta_+)\} - \eta(\sin 2\theta_2)/\epsilon_{zz}(\theta_2)] = 0; \\ -K(\theta_1)(d\theta/dz)_{z=-h} + \tfrac{1}{2}[B_{\theta-}\{\sin(2\theta_1 - 2\theta_-)\} - \eta(\sin 2\theta_1)/\epsilon_{zz}(\theta_1)] = 0; \end{aligned}\right\} \tag{8}$$

$$\eta = D_0(e_1 + e_3)/\epsilon_0. \tag{9}$$

For rigid anchoring of the director at the boundaries, W_S is removed from equation (7); then equation (8) is solved with boundary conditions

$$\theta(\pm h) = \theta_\pm. \tag{10}$$

The torque balance equation in the bulk contains D_0^2 while the polar term enters only the boundary conditions (balance of surface torque); $K(\theta)$ also shows how the curvature elastic constants get redefined by flexoelectricity.

It is convenient to solve equation (8) with (9) or (10) using the orthogonal collocation method [21] with the zeros of the 24th order Legendre polynomial [22] as collocation points. This enables us to calculate θ as a function of z. Then we can calculate average properties associated with the deformation. For instance [6, 7] if $v_{\parallel,\perp}$ are the principal refractive indices of the nematic then the effective or average refractive index of the sample

$$v_{\text{eff}} = (1/2h)\int_{-h}^{h} v_\perp v_\parallel \, dz \Big/ [v_\perp^2 C_\theta^2 + v_\parallel^2 S_\theta^2]^{1/2} \tag{11}$$

can be found numerically using Gaussian quadrature [22]. The next few sections will be devoted to a solution of the governing equations and calculation of average optical properties under different situations.

3. Solutions and results for the polar electrooptic effect

3.1. *Initial homogeneous alignment; $\theta_\pm = 0$*

In the absence of **E** and **H** the director is uniformly oriented along x. As long as V is below the Fréedericksz threshold, θ will remain zero in the sample and

$$D_z = \epsilon_0\epsilon_\perp E_{z0} = -\epsilon_0 V/2h, \tag{12}$$

where E_{z0} is the constant electric field inside the sample. Once V exceeds the threshold, a distortion as shown in equation (1) sets in and E_z becomes a function of z as given in equation (3); the simple relation (12) will no longer connect D_0 and V. Close to and just above the Fréedericksz threshold, however, we can assume that the deformation is small and linearize equations (8) and (9) with respect to θ. Then, to first order in the perturbations equation (12) will remain valid. The assumption that the distortion is small just above threshold is equivalent to stating that the Fréedericksz transition is one of second order; this will be justified subsequently by calculating the average deformation above the threshold. For the sake of completeness the splay Fréedericksz threshold will be calculated below.

Downloaded At: 11:44 26 January 2011

It is initially assumed that $H=0$. Then linearizing equations (8) and (9) with respects θ we get

$$\left.\begin{aligned} &\theta_{,\zeta\zeta}+Q^2\theta=0; \quad [\pm\theta_{,\xi}+\theta(\tau_\pm \mp \tau_e)]_{\xi=\pm 1}=0; \quad \xi=z/h; \\ &Q^2=\epsilon_A h^2 D_0^2/\epsilon_0\epsilon_\perp^2 K_1; \quad \tau_\pm = hB_{\theta\pm}/K_1; \quad \tau_\theta = D_0 h(e_1+e_3)/K_1\epsilon_\perp\epsilon_0. \end{aligned}\right\} \tag{13}$$

This eigenvalue is solved by the ansatz [13] $\theta=\theta_S \sin Q\xi+\theta_C\cos Q\xi$ which leads to the compatibility condition

$$[\tau_+\tau_- +\tau_e(\tau_+-\tau_-)-\tau_e^2-Q^2]\sin(2Q)+Q(\tau_++\tau_-)\cos(2Q)=0 \tag{14}$$

This condition can be rearranged to yield equation (49) of [13]. Once the value D_S of D_0 is found from equation (14) with $\epsilon_A>0$, the corresponding voltage V_S can be calculated from equation (12). The following qualitative conclusions can be arrived at by examining equation (14), remembering that the polar electric term enters only the boundary condition and not the torque balance equation for the bulk: (i) If $\tau_+=\tau_-$, then the magnitude of the Fréedericksz threshold is unchanged when the sign of τ_e is reversed. (ii) If $\tau_e=0$ (say, flexoelectricity is absent) then again the magnitude of the Fréedericksz threshold will remain unaltered under a change of sign of voltage even when the boundaries have different anchoring strengths. (iii) If $\tau_+\neq\tau_-$, then the Fréedericksz threshold will have different values for the two signs of V [13]. (iv) For rigid anchoring at both surfaces, $\tau_\pm\gg 1$ and $\sin 2Q=0$ yields the non-trivial estimate $\cos Q=0$ or $Q=\pi/2$ which leads to the correct expression for the splay threshold.

Including a magnetic field is straightforward. A field $\mathbf{H}_S=(H_S,0,0)$ along the x axis has a stabilizing influence for a material with $\chi_A>0$ and will consequently enhance the magnitude of the Fréedericksz threshold for a given sign of V; the threshold is calculated from equation (14) except that [23]

$$Q^2=[(\epsilon_A D_0^2/\epsilon_0\epsilon_\perp^2)-\mu_0\chi_A H_S^2](h^2/K_1). \tag{15}$$

Similarly a field $\mathbf{H}_D=(0,0,H_D)$ has a destabilizing influence and diminishes the electric threshold which is now found from equation (14) with

$$Q^2=[(\epsilon_A D_0^2/\epsilon_0\epsilon_\perp^2)+\mu_0\chi_A H_D^2](h^2/K_1). \tag{16}$$

In this case, however, equation (14) will be valid only for $H_D<$ the magnetic Fréedericksz threshold, H_F, which is found from

$$[\tau_+\tau_- -q^2]\sin(2q)+q(\tau_++\tau_-)\cos(2q)=0; \quad q^2=\mu_0\chi_A h^2 H_F^2/K_1. \tag{17}$$

Clearly, for rigid anchoring at both the surfaces, $q=\pi/2$ leads to the correct expression for the splay magnetic threshold.

To see the implications of the above results calculations are presented for a model nematic sample [14, 24] with the following parameters:

$$\left.\begin{aligned} &(K_1, K_3)=(1{\cdot}85, 2{\cdot}02)\times 10^{-12}\,\mathrm{N}; \quad (\epsilon_\parallel,\epsilon_\perp)=(18{\cdot}8, 5{\cdot}3); \\ &e_1+e_3=-0{\cdot}33\times 10^{-11}\,\mathrm{C\,m^{-1}}[11\text{–}13]; \quad 2h=3\,\mu\mathrm{m}; \quad \chi_A=4\pi\times 10^{-7}; \\ &v_\parallel=1{\cdot}724; \quad v_\perp=1{\cdot}513; \quad \lambda=0{\cdot}514\,\mu\mathrm{m}. \end{aligned}\right\} \tag{18}$$

All angles are measured in radians; the values of the flexoelectric coefficient and sample thickness are those given in equation (18) unless otherwise stated. To fix ideas, V_+ (or V_-) will refer to a positive (or a negative) potential difference as defined by equation (4).

Downloaded At: 11:44 26 January 2011

Plots of V_{S+} and V_{S-} are shown (see figure 1) as functions of $B_{\theta-}$ for a fixed value of $B_{\theta+} = 10^{-5}\,\mathrm{Nm}^{-1}$. The difference in the magnitudes of V_{S+} and V_{S-} becomes striking especially in the region of low $B_{\theta-}$. When the magnitude of the flexoelectric constants is doubled (see curves 3) the asymmetry becomes more pronounced; this becomes clearer in the presence of a magnetic field. While a stabilizing field $\mathbf{H}_S$ enhances the asymmetry (see figure 1 (*b*)) a destabilizing field $\mathbf{H}_D$ can even change the domain of stability of the initial director orientation when the sign of the applied voltage is reversed.

3.2. *Computation of the linear electrooptical effect*

Having obtained the threshold as detailed above, we consider fields higher than the threshold; using equations (8) and (9) the deformation angle $\theta(z)$ is calculated. For the initial homogeneous configuration we consider only one domain of distortion having a given parity; clearly, if $\theta(z)$ is a solution of equations (8) and (9), so is $-\theta(z)$. When the anchoring strengths at the two plates are different the $\theta(z)$ profile will be non-symmetric

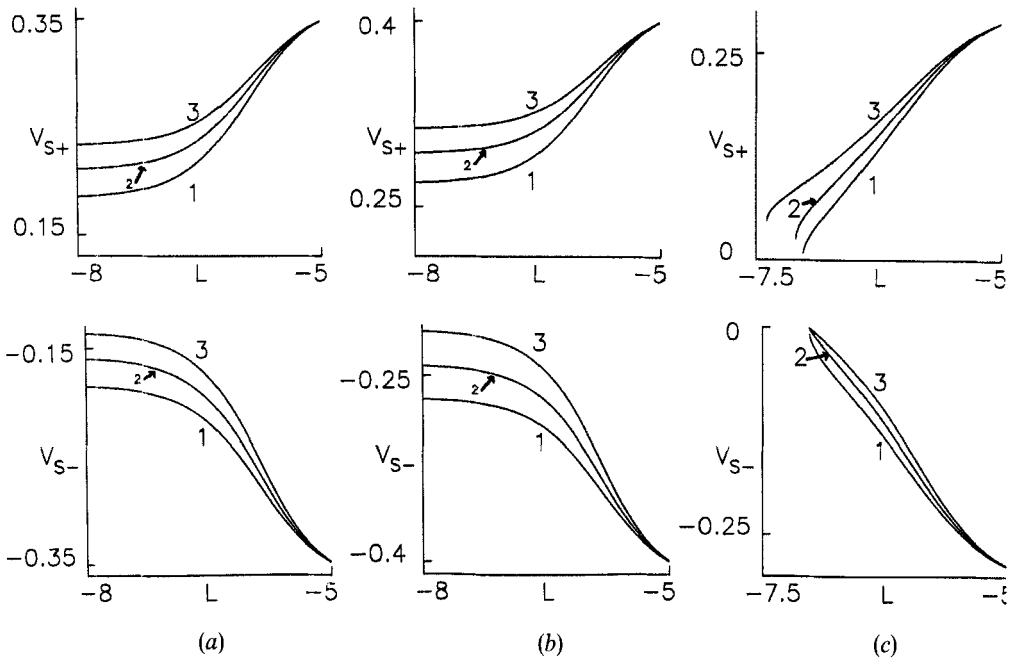

Figure 1. Plots of V_{S+} and V_{S-} as functions of $L = \log B_{\theta-}$ for $B_{\theta+} = 10^{-5}\,\mathrm{N\,m}^{-1}$. The initial director orientation is along x between plates $z = \pm h$ having director anchoring strengths $B_{\theta\pm}$, respectively. Sample thickness $2h = 3\,\mu\mathrm{m}$. $V_{S\pm}$ refer to positive and negative voltage, respectively, impressed on the sample in the sense of equation (4). The material parameters are as in equation (18). Curves have been drawn for $e_1 + e_3 = (1)\,0$, (2) $-0{\cdot}33 \times 10^{-11}$, (3) $-0{\cdot}66 \times 10^{-11}\,\mathrm{C\,m}^{-1}$. (*a*) The zero magnetic field case. The difference in the magnitudes of V_{S+} and V_{S-} is clearly noticeable when $B_{\theta-}$ becomes sufficiently small. (*b*) The effect of including a stabilizing magnetic field $\mathbf{H}_S$ along x with $H_S = 0{\cdot}5\,H_R$ where $H_R = (\pi/2h)(\chi_A/K_1)^{1/2}$ is the splay Fréedericksz threshold for rigid anchoring. (*c*) A destabilizing magnetic field $\mathbf{H}_D$ is included along z (normal to the sample planes) with $H_D = 0{\cdot}5H_R$. When $B_{\theta-}$ becomes sufficiently small the magnetic threshold H_F (found from equation (17)) can become smaller than H_R; this is why both V_{S+} and V_{S-} tend to zero when $B_{\theta-}$ diminishes beyond a certain limit. We can conclude that application of a magnetic field or enhancement of the flexoelectric coefficient can increase the difference between the magnitudes of V_{S+} and V_{S-} (see § 3.1).

Downloaded At: 11:44 26 January 2011

with respect to the sample centre with θ taking the extremum value θ_M at some point z_M, $-h < z_M < h$; θ_M can be regarded as a measure of the average deformation. In general, z_M will be closer to the plate having softer anchoring. The position of z_M can change when the applied voltage is reversed. A consequence of unequal anchoring strengths and flexoelectricity is that θ_2 and θ_1 will be different even when θ_+ and θ_- are equal.

Once the distortion profile has been calculated the optical phase difference between ordinary and extraordinary rays for a monochromatic radiation of wavelength λ can be found [6]:

$$\delta = (2\pi/\lambda)(2h)(v_{eff} - v_\perp), \tag{19}$$

where v_{eff} is defined in equation (11). This expresses the fact that as long as the director orientation is in the xz plane the extraordinary refractive index of the sample will diminish due to a deformation while the ordinary refractive index remains unchanged. If linearly polarized light is incident normal to the sample planes and if the angle between the plane of polarization and the initial director orientation is $\pi/4$, the ratio of transmitted intensity and incident intensity between crossed polaroids is given by [6]

$$R_I = \sin^2(\delta/2). \tag{20}$$

For a given $V_+ > V_{S+}$, $\delta(=\delta_+)$ and $R_I(=R_+)$ are determined. Suppose for $V_- = -V_+$ we calculate $\delta(=\delta_-)$ and $R_I(=R_-)$. Then

$$\Delta\delta = |\delta_+ - \delta_-|, \quad \Delta R = |R_+ - R_-| \tag{21}$$

give a measure of the polar electrooptic effect. The rest of § 3 deals with a study of ΔR as a function of different quantities.

3.3. *Results for* $\boldsymbol{H=0}$

Figure 2 contains plots of θ_M, δ and R as functions of V the magnitude of the voltage between the sample planes for two different cases of asymmetric anchoring. The anchoring strengths are chosen such that $(B_{\theta-}, B_{\theta+}) = (1,2) \times 10^{-5}\,\mathrm{N\,m^{-1}}$ (see figures 2(*a*)–(*c*)) are in the realm of relatively strong anchoring while $(B_{\theta-}, B_{\theta+}) = (1,2) \times 10^{-6}\,\mathrm{N\,m^{-1}}$ represent relatively weak director anchoring. Apart from the change in the Freedericksz threshold which is in agreement with [13], the following points may be noted:

(i) At sufficiently low V, the intensity of transmitted light should be less for V_+ than for V_-; $R_+ < R_-$.

(ii) At higher V this trend can reverse so that the two intensities can become equal at some intermediate voltages whose values obviously depend on the various parameters used; obviously at these voltages the linear electrooptic effect is extinguished.

(iii) The effect strengthens with weakening average anchoring strength (compare figures 2(*b*) and (*e*).

(iv) Similar curves have been drawn for $(B_{\theta-}, B_{\theta+}) = (2,3) \times 10^{-5}$ and $(2,3) \times 10^{-6}\,\mathrm{N\,m^{-1}}$ (these results have not been shown). This ensures that the difference in the anchoring strengths at the two boundaries remains the same though the average anchoring strength changes. Such calculations are useful for finding out whether a simple relationship exists between the magnitude of the effect and difference in anchoring strengths.

Downloaded At: 11:44 26 January 2011

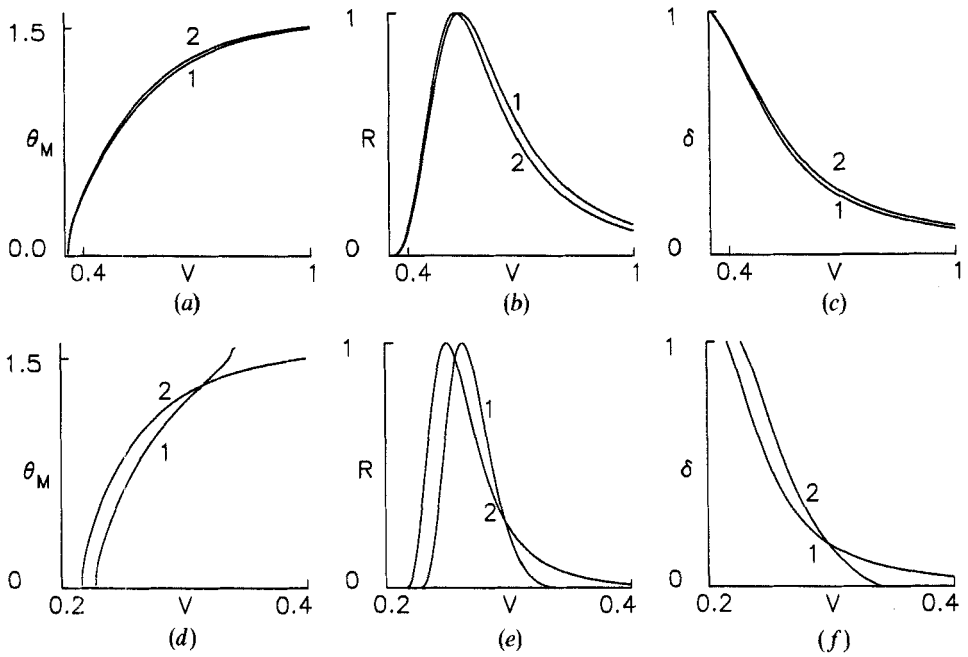

Figure 2. Plots of θ_M, $R_\pm$ and $\delta_\pm$ as functions of V, the magnitude of the potential difference between the plates $z = \pm h$. No applied magnetic field. Parameters are as in equation (18). Initial alignment is homogeneous along x. Due to asymmetry in anchoring, the extremum value θ_M of the deformation angle θ does not occur at the sample centre. R_I from equation (20) is the ratio of transmitted and incident intensities of plane polarized light normally incident on the sample planes; δ is the phase difference between the extraordinary and the ordinary rays in equation (19). The anchoring strengths are chosen to be $(B_{\theta-}, B_{\theta+}) = (a)$, (b) and (c) $(1{\cdot}0, 2{\cdot}0) \times 10^{-5}$, (d), (e) and (f) $(1{\cdot}0, 2{\cdot}0) \times 10^{-6}$ N m^{-1}. In the sense of equation (4), curves are drawn for (1) $V = V_+ > 0$, (2) $V = V_- < 0$. The changes occurring in δ and R_I under sign reversal of V are clearly manifest in (e) and (f) for weak average anchoring strength; equally apparent are the different magnitudes of the Fréedericksz threshold. R_I has a tendency to cross over when the sign of V is reversed showing that the polar electrooptic effect may be extinguished at some voltages. It may be noticed (see (d)) that curve 1 terminates at a fairly moderate value of $V(= V_A)$; at this point, θ in the sample $\rightarrow \pi/2$ with the director field tending to orient parallel to z in all parts of the sample. Curve 2 shows a similar tendency but at a higher magnitude of V_A. It appears (see § 3.7) that this can be regarded as a second order transition from a deformed state to the homeotropic and vice versa (see also the table). Due to the rather different domains of existence of the deformations for the two signs of the voltage, the magnitude of the electrooptic effect can be meaningfully computed only over their common range of existence (see § 3.2).

Curve 1 (see figures 2 (d)–(f)) is found to terminate at a relatively low voltage. At this point ($V_+ = V_{A+} \approx 0{\cdot}35$ V) where $\theta_M \rightarrow \pi/2$, there seems to be a tendency for the director field in all parts of the sample to align homeotropically (i.e. parallel to the applied field). Clearly at this point the orienting action of the substrates is completely overcome by the field. This is reminiscent of similar results [25] obtained for the transition from a hybrid aligned nematic to homeotropic orientation. For $V_+ > V_{A+}$ the θ_M versus V curve becomes simply a horizontal line and consequently curve 1 has been terminated at $V_+ = V_{A+}$. The same is found to occur for V_- but at a higher magnitude of $V_- = V_{A-} \approx -0{\cdot}5$ V; the trend is opposite to that shown by the Fréedericksz threshold. A

Downloaded At: 11:44 26 January 2011

look at equations (8) and (9) shows that this is due to flexoelectricity and asymmetric director anchoring. The magnitude of V_A remains unaltered under a sign reversal if the anchoring strengths are equal even though flexoelectricity is present; a qualitatively identical result is obtained if flexoelectricity is removed but the anchoring strengths are different. These points become more clear from the table.

At this stage it seems worth spending a little time over the actual mechanism which is at work. Consider what happens when an electric field is applied to a homogeneously aligned nematic. Above the Fréedericksz threshold a deformation sets in with θ taking an extremum θ_M at some point inside the sample. The distortion involves director gradients and the associated curvature elastic torque. This torque acts on the surface of the sample and tends to change the alignment of the director at the surface. If the anchoring is rigid then regardless of the deformation in the bulk the director orientation at the surfaces will be that dictated by the surface alignment. If, however, the anchoring energies at the two plates are finite the director orientation at the plates will change due to the action of the applied electric torque as well as the elastic torque; in the present case, the director orientation at the sample surfaces will change towards the homeotropic. When the electric field is sufficiently high we can think of a situation where the director field in the entire sample becomes homeotropic; beyond this stage, the director orientation will be unaffected by the field.

As the elastic torque exerted by the bulk on the surfaces falls off inversely as the square of the distance (note, for instance, the terms $d^2\theta/dz^2$ and $(d\theta/dz)^2$ in equation (8)), we can expect intuitively that if the sample becomes thicker a higher voltage will be necessary to orient the sample homeotropically; this is indeed seen to be the case from the table (note the values of $V_{A\pm}$ for a sample of thickness 6 μm).

The task that now presents itself is to compute ΔR and $\Delta\delta$ from different sets of data and plot them as functions of V. When the computation is done as described in § 2, it is not possible to get the mantissae for the same sets of the abscissae. Thus, for instance, if R_+ is known for $V_+ = +0{\cdot}31$ V, there may be no R_- value at exactly $V_- = -0{\cdot}31$ V. This is mainly because we start with given values of D_0 and calculate the potential

Downloaded At: 11:44 26 January 2011

V_S and V_A are, respectively, the splay Fréedericksz threshold and the orienting threshold for given director anchoring strengths $B_{\theta\pm}$ at the boundaries $z = \pm h$ ($2h$, the sample thickness, is measured in μm). The flexoelectric constant is $e_1 + e_3 = -0{\cdot}33 \times 10^{-11}$ C m^{-1} where applicable. $R_H = H/H_F$ where H_F is the splay magnetic threshold from equation (17). α (radian) is the angle made by **H** with the x axis in the xz plane.

	$(B_{\theta-}, B_{\theta+}) = (1, 2)\ 10^{-6}$/N m^{-1}				$(B_{\theta-}, B_{\theta+}) = (2, 3)\ 10^{-6}$/N m^{-1}			
	V_{S+}	V_{A+}	$-V_{S-}$	$-V_{A-}$	V_{S+}	V_{A+}	$-V_{S-}$	$-V_{A-}$
	$\theta_\pm = 0$ (homogeneous initial alignment); $R_H = 0$							
$2h = 3$	0·228	0·343	0·217	0·494	0·269	0·508	0·263	0·74
$2h = 6$	0·28	0·637	0·271	0·984	0·316	0·99	0·312	1·476
	$\theta_\pm = 0$ (homogeneous initial alignment); $R_H = 1$; $\alpha = 0$							
$2h = 3$	0·32	0·405	0·309	0·555	0·379	0·582	0·373	0·797
	$\theta_\pm = 0$ (homogeneous initial alignment); $R_H = 0{\cdot}5$; $\alpha = \pi/2$							
$2h = 3$	0·198	0·325	0·187	0·476	0·233	0·488	0·227	0·723
	$\theta_\pm = 0{\cdot}2$ (tilted initial alignment); $R_H = 0$; no Fréedericksz threshold							
$2h = 3$	—	1·64	—	1·686	—	1·786	—	1·824

difference from equations (8) and (4); when the sign of D_0 is reversed the distortion changes and hence the value of V calculated from equation (4) will have a different magnitude.

Hence the initial sets of data are used to generate data at the same set of intermediate points $V = V_+ = |V_-|$ over which non-trivial solutions for the distortions exist for both signs of the applied voltage; this is conveniently done by a linear interpolation if the initial sets of data have been obtained at sufficiently small intervals of V. Once this is done it is a simple matter to compute the magnitude of the polar electric effect—either ΔR or $\Delta\delta$.

Plots of ΔR and $\Delta\delta$ as functions of V are shown in figure 3. In all cases, ΔR is found to become zero at least once at some voltage above the Fréedericksz threshold; the magnitude of ΔR diminishes when the average anchoring strength is increased (compare figure 3 (*a*) with (*b*) and 3 (*c*) with (*d*)). In general, successive extrema have decreasing strength. There are, however, some qualitative differences between the strong and weak anchoring cases; in the former case (see figures 3 (*a*) and (*b*)), the second

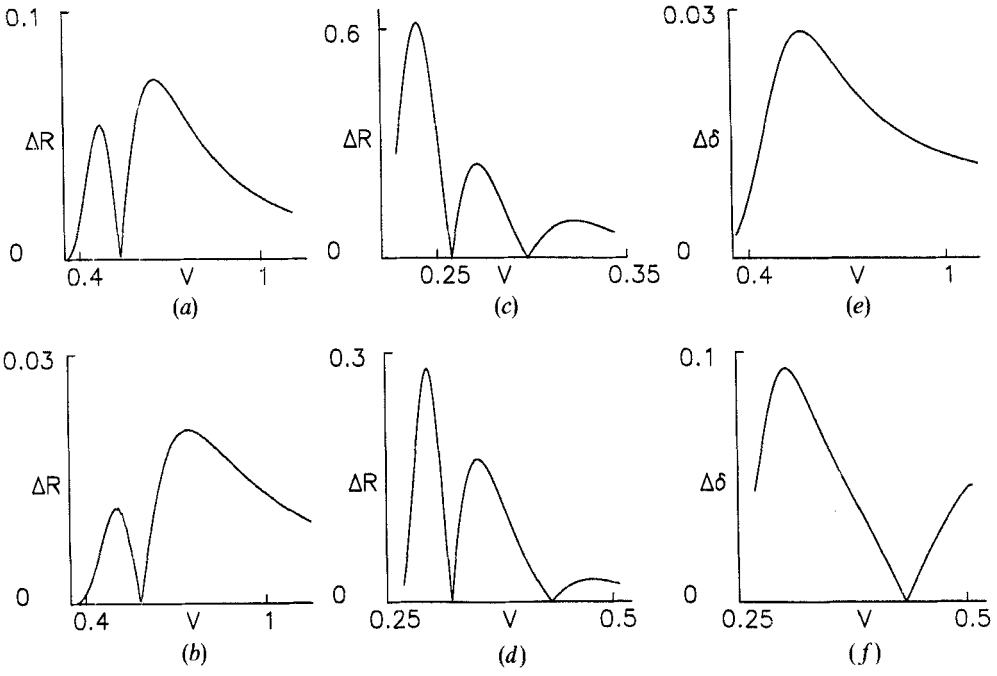

Figure 3. Variation of the magnitude of the linear electrooptic effect with the applied voltage $V = V_+ = |V_-|$ in the absence of a magnetic field. Initial homogeneous alignment. $\Delta\delta = |\delta_+ - \delta_-|$ where $\delta_\pm$ are the values of δ from equation (19) for $V_\pm$, respectively. Similarly, $\Delta R = |R_+ - R_-|$ where $R_\pm$ are the values of R_I from equation (20) for $V_\pm$, respectively. The figures are drawn for interfacial parameters $(B_{\theta-}, B_{\theta+}) =$ (*a*) and (*e*) (1·0, 2·0) $\times 10^{-5}$, (*b*) (2·0, 3·0) $\times 10^{-5}$, (*c*) (1·0, 2·0) $\times 10^{-6}$, (*d*) and (*f*) (2·0, 3·0) $\times 10^{-6}$ N m^{-1}. The magnitude of the effect generally diminishes with increasing average anchoring strength. For given $B_{\theta\pm}$, ΔR even goes to zero at some points above the Fréedericksz threshold and does not seem to depend only on the difference of anchoring strengths as shown to be true [14] at high enough voltages. We can discern certain qualitative differences between the strong anchoring ((*a*) and (*b*)) and the weak anchoring ((*c* and (*d*)) cases. When the flexoelectric constants are doubled (these curves are not included) these differences remain but the magnitude of the effect increases (see § 3.3).

Downloaded At: 11:44 26 January 2011

extremum of ΔR is the highest while in the latter case (see figures 3 (*c*) and (*d*)) the first extremum is the highest. In either case, there appears to be no simple relationship between ΔR and $|B_{\theta+} - B_{\theta-}|$, the difference in anchoring strengths, as found in the high voltage regime [14]. It is also found (curves have not been shown) that doubling the flexoelectric constants enhances the magnitude of the effect in every case; though the shapes of the curves are not appreciably altered the positions of extinction of the effect do change.

3.4. *The polar electrooptic effect in the presence of a magnetic field*

We consider only nematics with $\chi_A > 0$. In that case as long as **H** lies in the xz plane it is possible to restrict **n** also to lie in the same plane. While any tilt α of **H** is possible, it is convenient to consider in a preliminary effort either $\alpha = 0$ ($\mathbf{H} = \mathbf{H}_S$ is applied along x and is a stabilizing field) or $\alpha = \pi/2$ ($\mathbf{H} = \mathbf{H}_D$ is impressed along z and is a destabilizing field). A measure of the field strength is obtained in terms of H_F from equation (17).

Figures 4 (*a*) and (*b*) depict plots of ΔR for strong and weak anchoring. In each case a stabilizing magnetic field with strength $H_S = H_F$ is applied along x. Comparison of figures 4 (*a*) and (*b*) with the corresponding diagrams 3 (*a*) and (*d*) drawn for the case of zero magnetic field shows that the application of $\mathbf{H}_S$ tends to augment the magnitude of the effect and changes the positions of the extrema of ΔR as also the extinction voltages.

Downloaded At: 11:44 26 January 2011

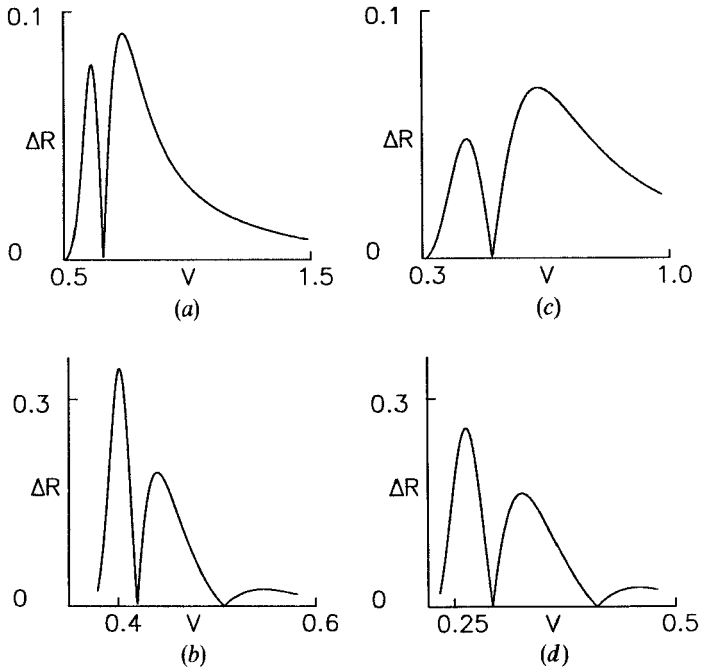

Figure 4. Influence of stabilizing ($\mathbf{H}_S$) and destabilizing ($\mathbf{H}_D$) magnetic fields on the variation of ΔR with V. Initial director orientation is homogeneous. $\mathbf{H}_S$ and $\mathbf{H}_D$ are applied, respectively, along x and z. The magnetic strength is measured in terms of H_F which is calculated from equation (17) for the given set of anchoring strengths $B_{\theta\pm}$. In (*a*) and (*b*), $H_S = H_F$ while in figures (*c*) and (*d*) $H_D = \frac{1}{2}H_F$. The interfacial parameters are $(B_{\theta-}, B_{\theta+}) =$ (*a*) and (*c*) $(1{\cdot}0, 2{\cdot}0) \times 10^{-5}$, (*b*) and (*d*) $(2{\cdot}0, 3{\cdot}0) \times 10^{-6}$ N m^{-1}. A stabilizing (or a destabilizing) magnetic field applied along (or normal to) the initial director orientation enhances (or diminishes) the magnitude of the effect. The application of a magnetic field also shifts the positions of the extrema as well as those of extinction (see § 3·4).

It is found (see table) that the magnitudes of $V_{S\pm}$ the splay Fréedericksz thresholds as also those of $V_{A\pm}$ the orienting thresholds increase due to $\mathbf{H}_S$.

It is straightforward to understand why the magnitude of the effect increases by examining equations (8) and (9). As remarked already, the origin of the effect is due to the presence of the linear electric term in the surface torques in equation (9). A stabilizing magnetic field essentially increases the effective splay electric threshold. As the effect is studied above the Fréedericksz threshold, the influence of the linear term in the surface torques is also enhanced.

By the same token, a destabilizing magnetic field $\mathbf{H}_D$ applied along z not only brings down the Fréedericksz thresholds $V_{S\pm}$ and the orienting thresholds $V_{A\pm}$ (see the table 1) but also diminishes the magnitude of the linear electrooptic effect. This is clearly manifest from a comparison of figures 4 (*c*) and (*d*) (drawn for $H_D=\frac{1}{2}H_F$) with figures 3 (*a*) and (*d*) (drawn for zero magnetic field). The qualitative argument follows closely that outlined in the previous paragraph. There occurs once more a repositioning of the extrema and points of extinction.

3.5. *Effect of sample thickness in the absence of a magnetic field*

We assume that $\mathbf{H}=0$ in this subsection. If the anchoring is rigid the solution of equation (8) and (10) leads to a sample thickness independent voltage threshold in the splay geometry. In this case, equation (8) can be cast into such a form that the effect of the electric field can be represented in terms of the reduced field $R_D=D_0/D_F$ where D_F is the threshold value. In this case the solution $\theta(z)$ will be the same at a fixed R_D for a given material and all sample thicknesses.

This scaling breaks down when the director anchoring at the plates is weak; in principle, therefore, the voltage threshold can be expected to be different for different sample thickness. One effect of increasing the sample thickness would be the occurrence of a greater number of extrema in the R versus V curves; this can certainly affect the nature of variation of ΔR with V. Another consequence of increasing the sample thickness is to decrease the elastic torque acting on the sample surfaces; essentially, therefore, this will have the effect of making the anchoring 'more rigid' for a given set of director anchoring strengths at the boundaries and this should be able to bring down the difference arising in the distortion due to change in the sign of the electric field—in other words, the magnitude of the polar electric effect should diminish. Another factor worth investigating is the voltage V_A at which the sample becomes homeotropic. From the arguments already given, it is seen that this voltage must increase with sample thickness.

A complete understanding of the influence of sample thickness will emerge only if calculations are done for a sufficient number of thicknesses; this falls outside the scope of the present work. In lieu of this a variation of the Fréedericksz thresholds $V_{S\pm}$ with sample thickness is presented in figures 5 (*a*) and (*b*). The anchoring at $z=+h$ is fixed at $B_{\theta\pm}=10^{-5}\,\mathrm{N\,m^{-1}}$; three different values of $B_{\theta-}$ are chosen. It is found that $V_{S+}\approx -V_{S-}$ when h is sufficiently high. When h is decreased to a low value there occurs a noticeable difference in the magnitudes of V_{S+} and V_{S-}; this is all the clearer when $B_{\theta-}$ is low enough.

Figures 5 (*c*)–(*f*) depict plots of ΔR versus V for a sample of thickness $2h=6\,\mu$m; the interfacial parameters are the same as those used in figures 3 (*a*)–(*d*) shows that when the sample thickness is increased the number of oscillations as well as the number of extinctions of ΔR increase. Going by the peak value of ΔR it is found that the

Downloaded At: 11:44 26 January 2011

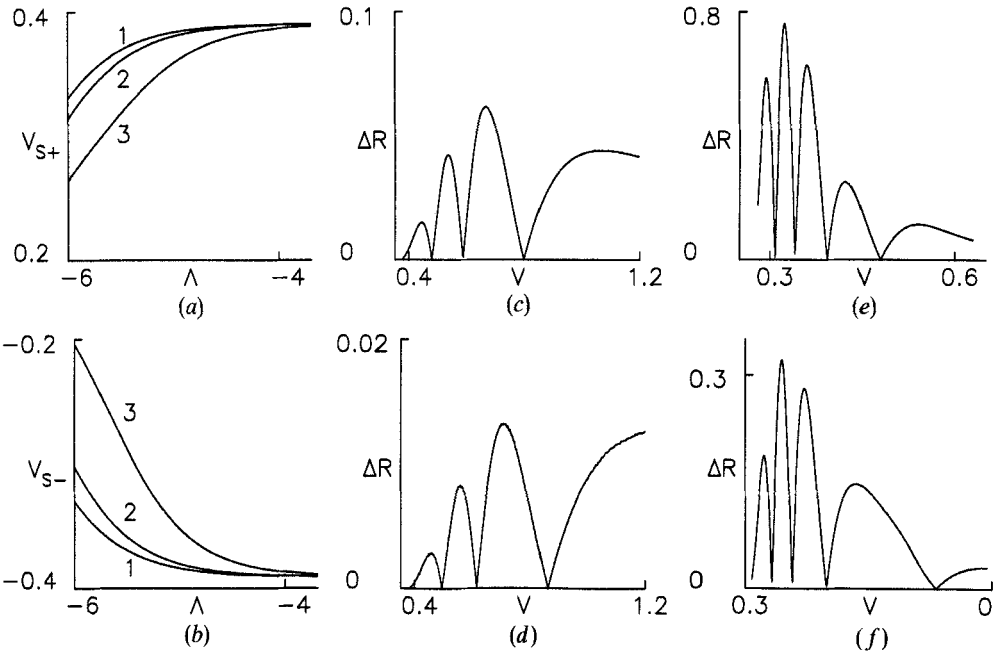

Figure 5. Effect of varying sample thickness. Initial director orientation is homogeneous. (*a*) and (*b*) plots of $V_{S\pm}$ as functions of $\Lambda = \log h$ where h is the semi-sample thickness. $B_{\theta+} = 10^{-5}\,\mathrm{N\,m^{-1}}$. Curves are drawn for $B_{\theta-} = (1) \times 10^{-5}$, (2) 5×10^{-6}, (3) $10^{-6}\,\mathrm{N\,m^{-1}}$. The magnitudes of $V_{S\pm}$ differ appreciably when the sample thickness is small enough and the anchoring sufficiently weak at one of the plates. (*c*)–(*f*) ΔR versus V for $2h = 6\mu$m. The anchoring strengths used are $(B_{\theta-}, B_{\theta+}) = (c)$ $(1{\cdot}0, 2{\cdot}0) \times 10^{-5}$, (*d*) $(2{\cdot}0, 3{\cdot}0) \times 10^{-5}$, (*e*) $(1{\cdot}0, 2{\cdot}0) \times 10^{-6}$, (*f*) $(2{\cdot}0, 3{\cdot}0) \times 10^{-6}\,\mathrm{N\,m^{-1}}$. These figures should be compared with figures 3 (*a*)–(*d*), respectively, drawn for $2h = 3\ \mu$m. It is seen that the number of oscillations as well as the number of extinctions increase with sample thickness. The peak amplitude of the effect diminishes (or increases) when the average anchoring is strong (or weak); see § 3.5.

magnitude of the effect diminishes for strong anchoring (see figures 5 (*c*) and (*d*) and 3 (*a*) and (*b*)) but increases for weak anchoring (see figures 5 (*e*) and (*f*) and 3 (*c*) and (*d*)). The augmentation in the magnitude of V_A has already been discussed and represented (see the table).

3.6. *Initial uniformly tilted alignment of the director:* $\theta_\pm = \theta_0 \neq 0$

We assume that $\mathbf{H} = 0$. The director is initially uniformly aligned in the xz plane making an angle θ_0 with the x axis. Obviously there is no electric Fréedericksz threshold in this configuration with the director field deforming under the action of even a small voltage (we can think of a magnetic threshold with $\mathbf{H}$ applied at an angle $\alpha = \theta_0 \pm \pi/2$ in the xz plane; this is a case which we do not consider here).

In figure 6, ΔR has been plotted as a function of the voltage for the same set of anchoring strengths as those used in figures 3 (*a*)–(*d*); a pretilt of $\theta_0 = 0{\cdot}2$ rad has been taken. It is instructive to compare figures 6 (*a*)–(*d*) with, respectively, figures 3 (*a*)–(*d*) (drawn for $\theta_0 = 0$). A significant diminution can be discerned in the magnitude of the polar electrooptic effect caused by changing the pretilt of the initial director orientation towards the homeotropic. This is compensated for by a slight increase in the voltage range over which the effect persists. The positions of the extrema and also those of the extinction of the effect get shifted.

Downloaded At: 11:44 26 January 2011

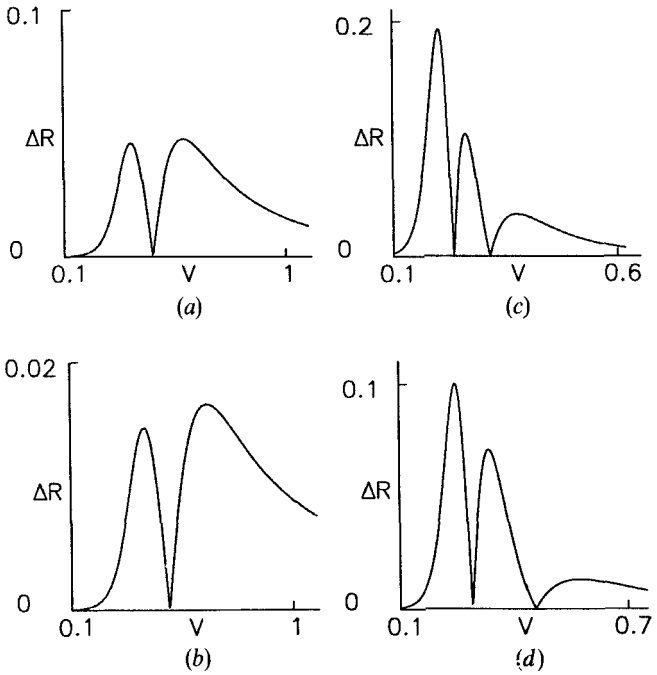

Figure 6. Effect of a uniform pretilt in the initial director orientation on the magnitude of the linear electrooptic effect. The director is tilted uniformly in the xz plane making an angle $\theta_0 = 0{\cdot}2$ rad with the x axis. All remaining parameters are the same as those used in figure 3. The non-existence of the electric Fréedericksz threshold in this case does lead to a small increase in the voltage range of the effect. A comparison of (*a*)–(*d*) with figures 3 (*a*)–(*d*), respectively, shows that the magnitude of the effect is diminished by the pretilt in both the strong (*a*) and (*b*)) and the weak ((*c*) and (*d*)) anchoring cases. The positions of the extrema and extinction are also shifted (see § 3.6).

In this case again when the applied voltage is sufficiently strong the director orientation in the bulk of the sample tends to the homeotropic. The values of $V_{A\pm}$ are shown in the table for $\theta_0 = 0{\cdot}2$ rad. It is found that while $|V_{A-}| > V_{A+}$ as in the remaining cases, the magnitudes of both $V_{A\pm}$ are much higher than those for the case of initial homogeneous alignment. Still, the magnitude of the effect becomes very small at higher voltages so that the magnitude of V_A does not cause an appreciable broadening of the voltage range over which the effect is significant. It is also found from the θ_M versus V curves (not included) that the transition to the complete homeotropic case occurs quite smoothly when the initial director orientation is pretilted. It will be shown presently that the estimate of V_A in this case cannot be made with the linear perturbation hypothesis.

A related case where an electric Fréedericksz threshold does not exist is that of the initial homogeneous orientation to which a magnetic field $\mathbf{H}_D$ is applied along z with $H_D > H_F$, the magnetic Fréedericksz threshold from equation (17). Here again, a director deformation exists even in the absence of an applied electric field. A sample calculation with $H_D = 1{\cdot}01\, H_F$ has been performed for the same set of anchoring strengths as those used in figures 3 and 6 (these results have not been included here). In this case again, even a small applied voltage can change the distortion in the sample and, in principle, we can compute the linear electrooptic effect right from the lowest possible voltage. A comparison with the corresponding figures 4 (*a*)–(*d*) shows that the

Downloaded At: 11:44 26 January 2011

magnitude of the effect is even lower than in the case of $H_D = 0{\cdot}5\,H_F$; in addition, the higher applied destabilizing field causes a lowering in the magnitude of V_A so that even the voltage range of existence of the effect gets curtailed.

3.7. Electric and magnetic thresholds for complete alignment of the sample

It has been seen already (see §3.3 and the table) that when the anchoring is sufficiently weak and the voltage exceeds a limit V_A the director orientation can become homeotropic in the entire sample. A similar observation can also be made by studying the θ profile as a function of an applied magnetic field. Suppose **H** is applied at $\alpha = \pi/2$ (along z). If H is increased beyond a certain limit H_A, the director orientation in the entire sample approaches $\pi/2$. As an example consider the case of equal, weak anchoring at the boundaries ($B_{\theta\pm} = 10^{-6}\,\mathrm{N\,m^{-1}}$) and the initial alignment is homogeneous ($\theta_\pm = 0$). Then for a sample thickness of $2h = 3\,\mu$m the ratio $r_A = H_A/H_F = 1{\cdot}3$ where H_F is the Fréedericksz threshold from equation (17). When the sample thickness is doubled ($2h = 6\,\mu$m) we find that $r_A = 1{\cdot}67$.

An attempt will be made below to evaluate these thresholds by a linear perturbation analysis of equations (8) and (9) under the assumption that $\theta(z) = (\pi/2) - \beta(z)$ where β is small; both electric and magnetic fields are assumed to act. The idea is to find out under what circumstances we obtain an eigenvalue equation. On linearizing with respect to β we get

$$\left.\begin{aligned}
&\beta_{,\xi\xi} - Q^2\beta = -\mu_0\chi_A h^2 H^2 S_\alpha C_\alpha / K_3;\\
&\qquad Q^2 = (D_0^2\epsilon_A/\epsilon_0\epsilon_\parallel^2)(h^2/K_3) \quad \text{if} \quad H = 0;\\
&\qquad Q^2 = [(D_0^2\epsilon_A/\epsilon_0\epsilon_\parallel^2) + \mu_0\chi_A H^2](h^2/K_3) \quad \text{if} \quad H \neq 0 \quad \text{and} \quad \alpha = \pi/2;\\
&\qquad Q^2 = [(D_0^2\epsilon_A/\epsilon_0\epsilon_\parallel^2) - \mu_0\chi_A H^2](h^2/K_3) \quad \text{if} \quad H \neq 0 \quad \text{and} \quad \alpha = 0;\\
&\qquad [\mp\beta_{,\xi} + \beta\{\mu_\pm(\cos 2\theta_\pm) \mp \mu_e\}]_{\xi=\pm 1} = -\tfrac{1}{2}\mu_\pm \sin 2\theta_\pm;\\
&\mu_\pm = B_{\theta\pm} h/K_3; \quad \mu_e = h(e_1 + e_3)D_0/\epsilon_0\epsilon_\perp K_3.
\end{aligned}\right\} \tag{22}$$

It is immediately seen that an eigenvalue equation will result only if $\theta_\pm = 0$ (initial homogeneous alignment) and $\alpha = 0$ (purely stabilizing magnetic field $\mathbf{H_S}$) or $\alpha = \pi/2$ (purely destabilizing magnetic field $\mathbf{H_D}$); as $\epsilon_A > 0$, we are not interested in $\theta_\pm = \pi/2$ (initial homeotropic alignment). A solution of equation (22) results in the compatibility condition

$$(\tanh 2Q)[Q^2 + (\mu_+ - \mu_e)(\mu_- + \mu_e)] - Q(\mu_+ + \mu_-) = 0 \tag{23}$$

from which the threshold D_A or $V_A = -2hD_A/\epsilon_0\epsilon_\parallel$ can be calculated (remembering that the director field is nearly homeotropic). It is clear from equation (23) that V_{A+} and V_{A-} will have different magnitudes for the same set of asymmetric anchoring strengths. The values of $V_{A\pm}$ calculated from equation (23) are in close agreement with those given in the table for initial homogeneous alignment. It appears, therefore, that in this case the transition to (from) the uniform homeotropic orientation from (to) the deformed state can be regarded as one of second order. When the applied electric field is zero ($D_0 = 0$) and $\alpha = \pi/2$, equation (23) can be solved to obtain the magnetic threshold H_A; the results are in good accordance with those obtained from the solution of equations (8) and (9).

For the sake of completeness it must be mentioned that when only a magnetic field is impressed ($D_0 = 0$), it is possible to generalize the above picture to include a uniformly pretilted alignment with $\theta_\pm = \theta_0$ and with $\alpha = \theta_0 + \pi/2$. In this case the Fréedericksz threshold $H_F(\theta_0)$ is found from equations (13) and (17) with K_1 being replaced by

Downloaded At: 11:44 26 January 2011

$K_1 \cos^2\theta_0 + K_3 \sin^2\theta_0$. The threshold $H_A(\theta_0)$ at which the director orientation goes over to $\theta(z) = \theta_0 + \pi/2$ is similarly obtained from equations (22) and (23) by replacing K_3 with $K_3 \cos^2\theta_0 + K_1 \sin^2\theta_0$. It is not intended to go into the details of this case.

4. Optical properties of bistable orientation patterns

It has been shown [19] that anchoring strengths at the sample boundaries have an important bearing not only on the magnetic field induced bistability width but also on the occurrence of bistability and the nature of the transition occurring near the edges of the bistable region. For the sake of simplicity it is assumed that the director anchoring at the surfaces is rigid from equation (10) and also that the initial director tilt is uniform ($\theta_\pm = \theta_0$) in the xz plane. We also neglect flexoelectricity for the moment as it affects only the bulk elastic torque in a non-polar fashion. In the absence of voltage the Fréedericksz threshold is obtained for $\alpha = \theta_0 \pm \pi/2$

$$H_f(\theta_0) = (\pi/2h)[(K_1 \cos^2\theta_0 + K_3 \sin^2\theta_0)/\mu_0\chi_A)^{1/2}. \tag{24}$$

When the initial director tilt is arbitrary there can exist no magnetic threshold in the presence of an electric field. But in two special cases we can obtain a magnetic threshold. When $\theta_0 = 0$ and $\alpha = \pi/2$

$$H_{f1} = (\pi/2h)[\{K_1 - (\epsilon_0\epsilon_A V^2/\pi^2)\}/\chi_A\mu_0]^{1/2}; \tag{25}$$

this expression which shows a reduction in the magnetic splay threshold due to the applied voltage is valid only for $V <$ the electric splay threshold. For $\theta_0 = \pi/2$ and $\alpha = 0$ we get, similarly,

$$H_{f2} = (\pi/2h)[\{K_3 + (\epsilon_0\epsilon_A V^2/\pi^2)\}/\chi_A\mu_0]^{1/2}; \tag{26}$$

the magnetic bend threshold is enhanced by the application of the stabilizing voltage.

We shall first consider the case of zero electric field. The solutions of interest are those which represent deformations occurring in the sample when the magnetic tilt α is changed in small steps starting from either end of the range $\theta_0 \leqq \alpha \leqq \theta_0 + \pi$. The distortion at any magnetic tilt will be symmetric with respect to the sample centre with $\theta(z)$ taking an extremum value θ_M at $z = 0$. The aim is now to study θ_M as a function of α as it is well-known [17–19] that the nature of variation of θ_M with α depends strongly on the reduced field $r_H = H/H_f$.

Figure 7 (*a*) depicts a typical set of curves obtained for $\theta_0 = 1{\cdot}17$ rad. When $r_H < 1$, θ_M is a continuous, single valued function of α. For $r_H = 1$, θ_M shows a small jump as α crosses $\theta_0 + \pi/2$. When $r_H > 1$, the curve splits into two branches overlapping over a range of α called the bistability width which generally increases with r_H. For α in the bistable region it is possible to have two distinct deformation states having different free energies, each state resulting from the particular history of α variation. When α is varied beyond the edges of the bistable region a discontinuous transition can be observed [17, 18] from the higher energy distortion state to the one having lower energy.

It is worth noting that the shape of the θ_M curves shows a certain symmetry relative to the centre of the α range—one branch can be got from the other by a suitable reflection. When the initial pretilt of the director is symmetric relative to the sample centre ($\theta_0 = 0$ or $\pi/2$) the deformation states equidistant from the midrange will contain equal amounts of splay and bend. On the other hand when θ_0 takes some arbitrary value it becomes clear that the deformation which results by varying α from θ_0 can have quite a different character as compared to that resulting from a variation of α from $\theta_0 + \pi$; in the former case. θ_M starts increasing towards the homeotropic value ($\pi/2$) while in

Downloaded At: 11:44 26 January 2011

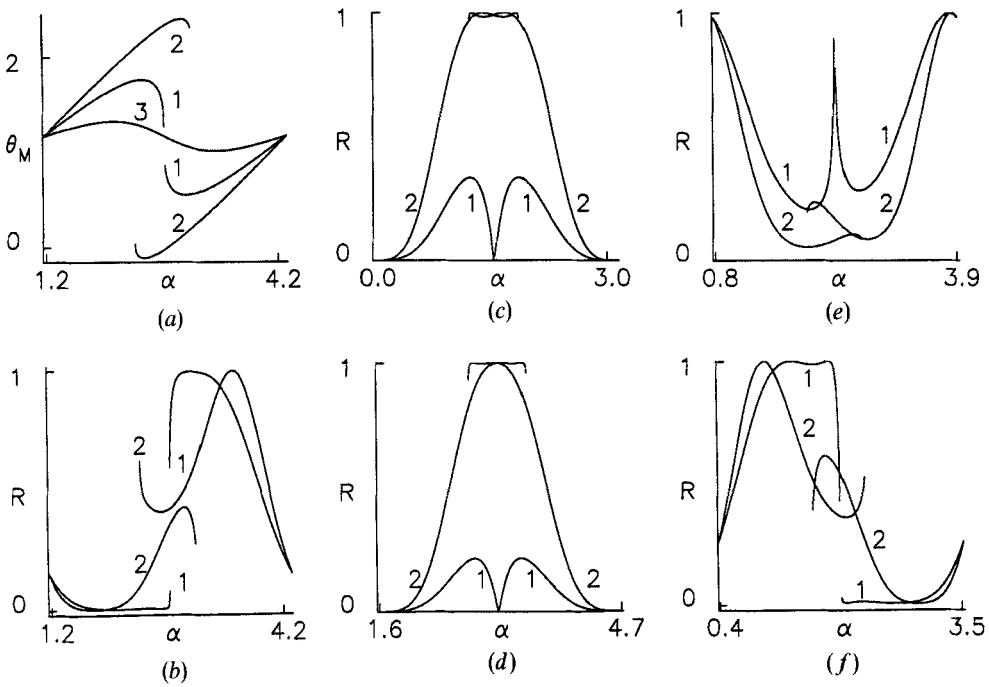

Figure 7. The variations of average distortion and transmitted intensity with the magnetic tilt angle α for rigid anchoring of the director at the boundaries in the absence of an electric field. The initial director orientation is uniformly tilted making an angle θ_0 with the x axis in the xz plane. The magnetic field **H** is rotated in small steps in the xz plane from the end points of the range $\theta_0 \leqq \alpha \leqq \theta_0 + \alpha$. The reduced field $r_H = H/H_f$ where H_f is the Fréedericksz threshold from equation (24). The deformation is symmetric with $\theta(z)$ taking the extremum value θ_M at the sample centre $z = 0$. Sample thickness $2h = 3$ μm. Curves are drawn for $r_H = (1)$ 1·0, (2) 1·5, (3) 0·5. (*a*) θ_M versus α for $\theta_0 = 1{\cdot}17$ rad. Curves for other θ_0 have similar shapes; each branch of a given curve can be got from the other by a suitable reflection in the centre of the α range. (*b*)–(*f*) R versus α for $\theta_0 = (b)$ 1·17, (*c*) 0·0, (*d*) $\pi/2$, (*e*) 0·78, (*f*) 0·39. R is proportional to the intensity of light transmitted between crossed polarizers. Only for $\theta_0 = 0$ and $\pi/2$ (*c*) and (*d*) is the variation of R symmetric with respect to $\alpha = \theta_0 + \pi/2$; in all other cases the variation of R is asymmetric. There may occur oscillations in the R variation for thicker samples (see § 4).

the latter case θ_M initially diminishes towards the homogeneous value. Due to the birefringence of the medium this difference in distortion should be reflected in the optical properties of the sample.

Figures 7 (*b*)–(*f*) represent the transmitted intensity R as a function of α for different director pretilts. The results obtained for a sample thickness of 3 μm show that while the curves show a symmetry relative to the centre of the α range in the case of homogeneous and homeotropic alignments ((*c*) and (*d*)), a lack of symmetry is discernible in the others ((*b*), (*d*) and (*f*)).

In the presence of an applied electric field the calculations are not so straightforward. In an experiment it is convenient to impress a magnetic field of some strength at, say, $\alpha = \theta_0$ and then apply a voltage V across the sample. Keeping V fixed, the tilt of **H** can be changed and the variations of different properties with the magnetic tilt studied. From the viewpoint of a theoretical calculation it is seen from equation (5) that every time α is changed there occurs a corresponding change in the distortion and in order

Downloaded At: 11:44 26 January 2011

that V may be obtained at a constant value, D_0 has to be altered; in other words, D_0 becomes a function of α for a given V and r_H. Every time α is varied, D_0 has to be determined by iteration such that V remains constant. It must be remembered that as we neglect flexoelectricity, its volume contribution to $K(\theta)$ vanishes; in addition, the function ψ in equation (5) will remain zero.

As stated earlier, an applied voltage has a destabilizing influence on the homogeneous alignment and leads to a lowering of the effective magnetic splay threshold H_{f1} from equation (25). An obvious consequence of this is that if we start with a reduced field $r_H < 1$ and include a sufficiently high electric field along z, bistability should result when α is varied from the two ends of its range, $0 \leqq \alpha \leqq \pi$. This is indeed found to be the case. For instance, with $r_H = H/H_f(0) = 0{\cdot}5$, $V = 0$, θ_M varies continuously with α while with $V = 0{\cdot}4$ V, bistability results in the single curve breaking up into two branches. The θ_M and R curves are similar in shape to those given in figures 7 (*a*)–(*d*) and have not been shown.

A similar result is obtained when the initial orientation is homeotropic. In this case an applied voltage enhances the effective bend magnetic threshold H_{f2} from equation (26). It is, therefore, natural that the bistability that occurs for a given $r_H > 1$ should be

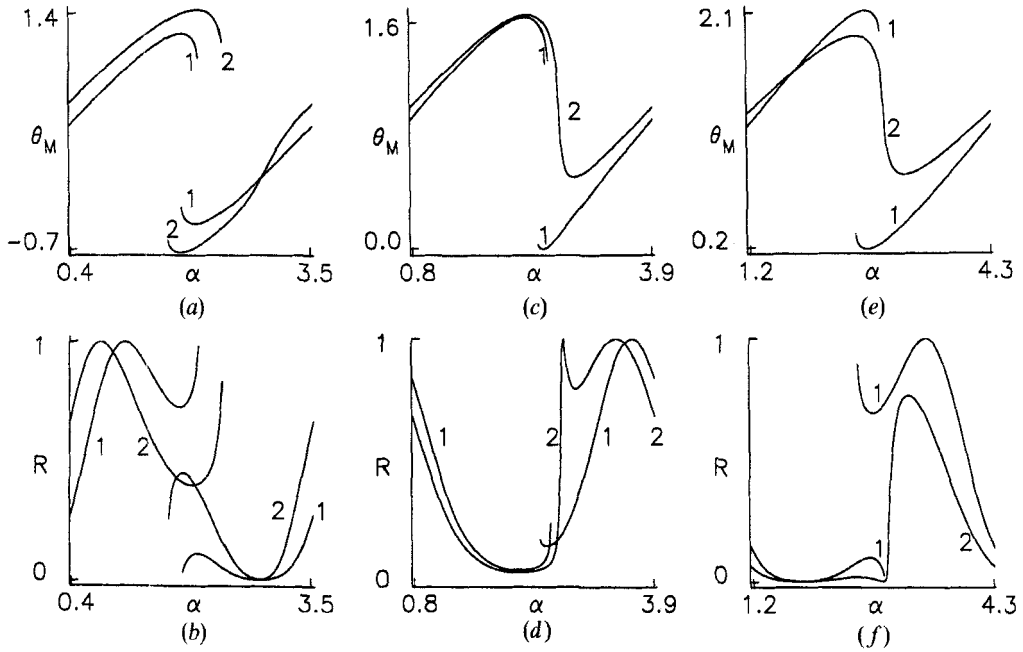

Figure 8. The variation of average distortion and transmitted intensity as functions of the magnetic tilt angle α for rigid anchoring at the boundaries in the presence of an applied voltage V. The initial director orientation is uniform in the xz plane making an angle θ_0 with the x axis. $\theta_0 =$ (*a*) and (*b*) 0·39, (*c*) and (*d*) 0·78, (*e*) and (*f*) 1·17 rad. The reduced magnetic field $r_H = H/H_f(\theta_0)$ where H_f is the magnetic Fréedericksz threshold (for zero electric field); $r_H =$ (*a*) and (*b*) 1·2, (*c*) and (*d*) 1·2, (*e*) and (*f*) 1·3. The applied voltage between the sample planes is $V =$ (1) 0·1, (2) 0·4 in (*a*) and (*b*); $V =$ (1) 0·3, (2) 0·4 in (*c*) and (*d*); $V =$ (1) 0·1 (2) 0·4 in ((*e*) and (*f*)). Depending upon θ_0, an applied electric field either enhances (*a*) and (*b*) or diminishes (*c*)–(*f*) the bistability width at a given reduced magnetic field. Wjen θ_0 is sufficiently close to the homeotropic bistability it may even disappear (see curves 2, (*c*)–(*f*)) under the action of a strong electric field. The presence of the electric field also destroys the symmetry of the θ_M curves and causes qualitative changes in the nature of variation of R (see § 4).

Downloaded At: 11:44 26 January 2011

suppressed by the application of a sufficiently high voltage V. It is found, for example, that bistability for $r_H = H/H_f(\pi/2) = 1{\cdot}3$ can be eliminated by using $V = 0{\cdot}4$ V. Again the curves have not been included as their shapes are similar to those in figures 7 (*a*)–(*d*).

When θ_0 takes arbitrary values we can discern certain qualitative changes in the shapes of the curves (see figure 8). When θ_0 is sufficiently close to zero (see figure 8 (*a*)) application of V causes the bistability width to increase. When θ_0 is high enough (see figures 8 (*c*) and (*e*)) the effect of impressing an electric field is to either reduce the bistability width or erase the occurrence of bistability altogether. What should be noted, however, is the lack of symmetry in the θ_M variation with respect to the centre of the α range (compare with figure 7 (*a*)). It is also seen, especially for $\theta_0 = \pi/4$ (compare figures 8 (*d*) and 7 (*e*)), that the shape of the R versus α curves also changes considerably under the action of an electric field. The results of figures 7 and 8 are capable of being checked experimentally.

5. Conclusions, limitations of the present work and possible extensions

When the sample surfaces of a nematic cell have unequal director anchoring strengths the director deformation produced by an electric field acting normal to the sample planes as well as the average optical properties change under sign reversal of the voltage due to flexoelectricity; this change provides a convenient way to visualize the polar electric effect involved [13, 14]. With initial homogeneous orientation in the sample the magnitude of the Fréedericksz threshold (V_S) also shows polarity dependence [13].

In this work the above effect has also been studied in the voltage region close to the Fréedericksz thresholds. It is seen from equations (5)–(8) that a reversal in the signs of D_0 and the flexoelectric constants leaves the equations invariant. It is, therefore, considered sufficient to study the modulus of the effect in equation (21) leaving finer details regarding the sign.

The magnitude of the effect can be enhanced (or diminished) by applying a stabilizing (or destabilizing) magnetic field along (or normal) to the initial homogeneous orientation. The effect becomes weaker with increasing sample thickness or with a change of initial director tilt away from the homogeneous. The effect can vanish at discrete values of the voltages for a given sample thickness; the number of these extinctions should depend on the optical parameters and sample thickness. Unlike at high voltages [14], the magnitude of the effect is not simply dependent on the difference in anchoring strengths close to the threshold.

When the anchoring strengths are sufficiently low the application of a high enough voltage (V_A) causes **n** to become homeotropic in the sample. With initial homogeneous orientation this can be regarded as a second order phase transition. In the presence of flexoelectricity, the magnitude of V_A is also polarity dependent. The application of a stabilizing (or destabilizing) magnetic field should enhance (or diminish) $|V_A|$. In the absence of voltage, a magnetic field **H** applied normal to the plates can also cause a transition to the homeotropic alignment if $H > H_A$; in this case field polarity is irrelevant.

Magnetic field induced bistability under the action of an applied electric field for rigid director anchoring at the boundaries is studied. The presence of the electric field can either enhance the bistability width or suppress the occurrence of bistability depending upon the initial director orientation. In addition, the electric field can profoundly affect the nature of variation of the average optical properties with magnetic tilt. Many results of this work are capable of experimental verification.

Downloaded At: 11:44 26 January 2011

Some of the limitations of the present work must be clearly stated. The material is assumed to have $\epsilon_A, \chi_A > 0$. This naturally narrows down the range of phenomena that can be studied from a qualitative viewpoint. It has not been possible to recover the results of [14] in the high voltage regime for strong director anchoring. This is because at such fields the computation by the usual methods can become somewhat inaccurate and we have to resort to special algorithms (see, for instance, [26]). The influence of changing sample thickness also needs to be studied in greater detail.

The distortion is assumed to depend on only one space coordinate (z); this naturally excludes the possibility of including domains containing deformation of opposite parity. The formation of domains cannot be ruled out especially in the Fréedericksz geometries. It should be interesting to study how the nature of domain formation is affected by changing the polarity of the applied voltage when the sample boundaries have different anchoring strengths.

Only deformations depending on one distortion angle have been studied in the present work. It has been shown [19] that the occurrence of bistability as well as the bistability width are strongly influenced in cases where the director deformation is described by two degrees of freedom. These situations arise either when the initial deformation has an intrinsic twist or when the magnetic plane makes an arbitrary angle with the sample planes or in materials having $\chi_A < 0$. It should be interesting to study how the optical properties of such distortions change with magnetic tilt, especially under the influence of an electric field.

Even in the electric splay geometry with dissimilar boundaries the application of an oblique magnetic field (**H** lying in the yz plane normal to x the initial homogeneous orientation) can bring in not only the twist angle of distortion but also the (unequal) twist anchoring strengths; the polar effect at, as well as above, the electric threshold can be expected to be influenced by the presence of **H** in the yz plane.

Only the effect of **H** applied along x or along z has been studied in the present work for weak anchoring at the boundaries. The influence of **H** impressed along arbitrary directions in the xz plane can be quite striking [19] especially when the anchoring strengths are small and the field strong enough; for a given H a discontinuous transition can be expected from a homogeneously deformed state to one in which the director alignment is along **H** when the magnetic angle is changed beyond some limiting value. It should be instructive to find out how the deformation changes with magnetic tilt in the presence of an electric field when the anchoring strengths are unequal.

The material has been assumed to be an insulator. In general nematic materials possess anisotropic electrical conductivity which leads to electrohydrodynamic instabilities in many cases [4–6]. Even in situations where such instabilities cannot set in it is known [7, 10] that the nature of the electric field induced distortion can be affected by the presence of conductivity. Conductivity may become particularly important for another reason. It is now known [27] that the presence of charges in a nematic sample can drastically affect the anchoring strengths in some cases. Considering that the polar electric effect owes its origin to both flexoelectricity and unequal anchoring strengths it seems necessary to study the influence of electrical conductivity on the effect.

The expression for the homeotropic aligning voltage, V_A, has been obtained from a linear perturbation analysis which is strictly valid only under certain restrictions (see § 3.7). In general it will be necessary to resort to a Landau expansion to get estimates of V_A.

Downloaded At: 11:44 26 January 2011

Lastly it must be remembered that all calculations have been done with a static electric field. One possible consequence of using a time varying or AC electric field would be to affect the effective flexoelectric contribution; (for instance the term $-P_iE_i$ in the total free energy). If the AC field has a period much lower than the director relaxation time it is quite likely that the flexoelectric contribution will average out to zero. It seems interesting to study the effect of AC field frequency on nematic samples with asymmetric surface treatment.

The author thanks a referee for useful comments on a previous version of the manuscript.

References

[1] OSEEN, C. W., 1933, *Trans. Faraday Soc.*, **29,** 883.
[2] FRANK, F. C., 1958, *Discuss. Faraday Soc.*, **25,** 19.
[3] ERICKSEN, J. L., 1976, *Advances in Liquid Crystals*, edited by G. H. Brown (Academic Press), p. 233.
[4] DE GENNES, P. G., 1975, *The Physics of Liquid Crystals* (Clarendon Press), Chap 3.
[5] CHANDRASEKHAR, S., 1977, *Liquid Crystals* (Cambridge University Press), Chap. 3.
[6] BLINOV, L. M., 1983, *Electrooptical and Magnetooptical Properties of Liquid Crystals* (Wiley), Chap. 4.
[7] DEULING, H. J., 1978, *Solid St. Phys. Suppl.*, **14,** 77.
[8] MEYER, R. B., 1969, *Phys. Rev. Lett.*, **22,** 918.
[9] RAPINI, A., and PAPOULAR, M., 1969, *J. Phys., Paris, Colloq.*, **30,** C4–54; GUYON, E., and URBACH, W., 1976, *Non-emissive Electrooptic Displays*, edited by A. R. Kmetz and F. K. von Willisen (Plenum Press), p. 121.
[10] DOZOV, I., BARBERO, G., PALIERNE, J. F., and DURAND, G., 1986, *Europhysics Lett.*, **1,** 563.
[11] SCHMIDT, D., SCHADT, M., and HELFRICH, W., 1972, *Z. Naturf.* (*a*), **27,** 277; HELFRICH, W., 1974, *Appl. Phys. Lett.*, **24,** 451.
[12] PROST, J., and PERSHAN, P. S., 1976, *J. appl. Phys.*, **47,** 2298; DOZOV, I., MARTINOT-LAGARDE, PH., and DURAND, G., 1982, *J. Phys. Lett., Paris*, **43,** L–365; 1983, *J. Phys. Lett., Paris*, **44,** L–817.
[13] DERZHANSKI, A., PETROV, A. G., and MITOV, M. D., 1978, *J. Phys., Paris*, **39,** 273.
[14] LEE, S-D., PATEL, J. S., 1990, *Phys. Rev. Lett.*, **65,** 56; 1990, *Mod. Phys. Lett.*, B, **4,** 1071.
[15] FRISKEN, B. J., and PALFFY-MUHORAY, P., 1989, *Phys. Rev.* A, **39,** 1513; 1989, *Ibid.*, **40,** 6099.
[16] KINI, U. D., 1990, *Liq. Crystals*, **8,** 745.
[17] ONNAGAWA, H., and MIYASHITA, K., 1974, *Jap. J. appl. Phys.*, **13,** 1741; MOTOOKA, T., and FUKUHARA, A., 1979, *J. appl. Phys.*, **50,** 3322.
[18] KARN, A. J., and SHEN, Y. R., 1990, *Phys. Rev.* A, **41,** 4510.
[19] KINI, U. D., 1991, *Liq. Crystals*, **10,** 597; 1992, *Liq. Crystals*, **12,** 449.
[20] LANDAU, L. D., LIFSHITZ, E. M., and PITAEVSKI, L. P., 1984, *Electrodynamics of Continuous Media* (Pergamon), Chap. II.
[21] FINLAYSON, B. A., 1972, *The Method of Weighted Residuals and Variational Principles* (Academic Press), Chap. 5; TSENG, H. C., SILVER, D. L., and FINLAYSON, B. A., 1972, *Phys. Fluids*, **15,** 1213.
[22] ABRAMOWITZ, M., and STEGUN, I. A. (editors), 1972, *Handbook of Mathematical Functions* (Dover), p. 916.
[23] GRULER, H., SCHEFFER, T. J., and MEIER, G., 1972, *Z. Naturf.* (*a*), **27,** 966; BARBERO, G., MALVANO, R., and STRIGAZZI, A., 1980, *Nuovo Cim.* B, **59,** 367.
[24] BERREMAN, D. W., 1980, *The Physics and Chemistry of Liquid Crystal Devices*, edited by G. J. Sprokel (Plenum Press) p. 1.
[25] HOCHBAUM, A., and LABES, M. M., 1982, *J. appl. Phys.*, **53,** 2998; BARBERO, G., and BARBERI, R., 1983, *J. Phys., Paris*, **44,** 609.
[26] WELFORD, K. R., and SAMBLES, J. R., 1987, *Molec. Crystals liq. Crystals*, **147,** 25.
[27] BARBERO, G., and DURAND, G., 1990, *J. appl. Phys.*, **67,** 2678.

Downloaded At: 11:44 26 January 2011